Chiral Surfaces

DOI: 10.1002/anie.201209025

Enantioselective Separation on Naturally Chiral Metal Surfaces: D,L-Aspartic Acid on Cu(3,1,17)$^{R\&S}$ Surfaces**

Yongju Yun and Andrew J. Gellman*

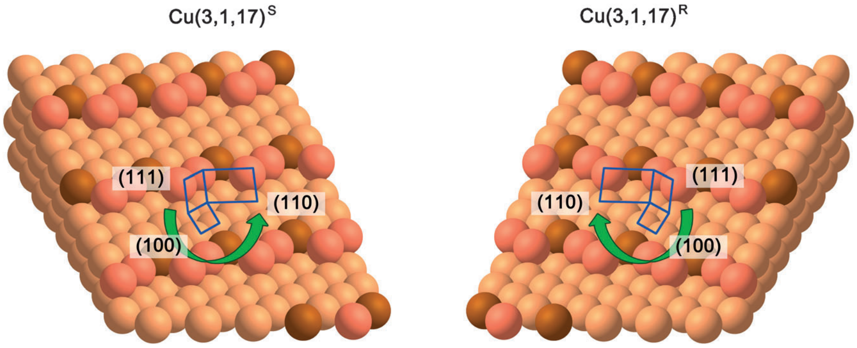

Figure 1. Ball model depiction of the Cu(3,1,17)$^{R\&S}$ chiral single-crystal surfaces. The Cu(3,1,17)$^{R\&S}$ surfaces have kinked steps formed by (110) and (111) microfacets, separated by (100) terraces. The enantiomorphous surfaces are nonsuperimposable because the three microfacets forming each kink have opposite rotational orientation. The kinked structures with a clockwise and counterclockwise rotation, (111)→(100)→(110), are designated *R* and *S*, respectively.

Homochirality of amino acids, sugars, proteins, and DNA is one of the biochemical hallmarks of life on Earth.[1] Its origins have been debated for decades. Given that minerals such as quartz were probably the first enantiomerically pure materials on Earth, it has been suggested that such materials served as chiral substrates for enantiospecific surface chemistry. Enantiospecific adsorption on the naturally chiral surfaces of minerals has been demonstrated, however, the enantiomeric excesses have been only 1–2 % with a couple of examples suggesting enantiomeric excesses of ca. 10 %.[1,2] Higher enantioselectivities have been observed for adsorption on chiral surfaces of organic crystals.[3] Highly enantioselective adsorption could be of enormous importance, if observed on catalytically active materials such as metals. Herein, we demonstrate that naturally chiral metal surfaces can yield much higher enantioselectivities than minerals and we provide the first definitive proof of enantioselective separation by a naturally chiral metal surface.

Chiral surfaces can be created by adsorption of chiral molecules on achiral substrates or by cleavage of crystals with bulk chiral structures.[1,2,4] Somewhat counter-intuitively, chiral surfaces can also be generated from achiral materials such as metals.[5] As an example, the two non-superimposable mirror images of the Cu(3,1,17) surface are illustrated in Figure 1. The kinked step structures of these surfaces lack symmetry and, therefore, they are chiral. The first experimental observation of enantioselectivity on naturally chiral surfaces used cyclic voltammetry measurements to show that L-glucose oxidizes more rapidly than D-glucose on the Pt(643)^S surface, and vice versa on Pt(643)^R.[5b,c] Gellman et al. showed that the enantiospecific desorption kinetics of *R*-3-methylcyclohexanone from chiral Cu(643)$^{R\&S}$ surfaces can result in a kinetic separation of 3-methylcyclohexanone.[5d,f]

A fundamental challenge in enantioselective surface chemistry and catalysis is to understand the molecular origins of enantioselectivity. The enantiospecific interactions between chiral molecules and chiral surfaces manifest themselves in enantiospecific differences in adsorption energetics and reaction kinetics. Thus, detection of enantiospecificity on chiral surfaces is the first step toward understanding the origins of enantioselectivity. However, such work has been hampered by the difficulty in differentiating two adsorbed enantiomers. Early work made use of different radioisotopes in the two enantiomers.[2b,f] Here, we demonstrate the use of ^{13}C labeling for enantiodiscrimination of chiral adsorbed species. Enantioselective separation of gas phase D,L-aspartic acid by equilibrium adsorption on naturally chiral Cu(3,1,17)$^{R\&S}$ surfaces was demonstrated and quantified by measuring the ratios of the enantiospecific adsorption equilibrium constants, $K_S^{\mathrm{D}}/K_S^{\mathrm{L}} = K_R^{\mathrm{L}}/K_R^{\mathrm{D}}$.

Measurements of adsorption isotherms (adsorbate coverage as a function of pressure at constant temperature, $\theta(P)\,|_T$) can be used to determine adsorption equilibrium constants and adsorption free energies. As illustrated in Figure 2, exposure of a racemic mixture of D- and L-enantiomers to the *R*- or *S*-enantiomers of a chiral surface results in the adsorption of non-racemic mixtures onto the surfaces. The relative coverages of the enantiomers, $\theta_S^{\mathrm{D}}/\theta_S^{\mathrm{L}} = \theta_R^{\mathrm{L}}/\theta_R^{\mathrm{D}}$, then provide quantitative measurements of the enantiospecific difference in the adsorption free energy: $\Delta\Delta G = \Delta G_S^{\mathrm{D}} - \Delta G_S^{\mathrm{L}} = \Delta G_R^{\mathrm{L}} - \Delta G_R^{\mathrm{D}}$.

---

[*] Y. Yun, Prof. A. J. Gellman
Department of Chemical Engineering, Carnegie Mellon University
5000 Forbes Ave., Pittsburgh, PA 15213 (USA)
E-mail: gellman@cmu.edu
Homepage: http://www.cheme.cmu.edu/people/faculty/ag4b.htm

[**] We thank the US DOE for support through Grant No. DE-FG02-12ER16330.

Supporting information for this article is available on the WWW under http://dx.doi.org/10.1002/anie.201209025.

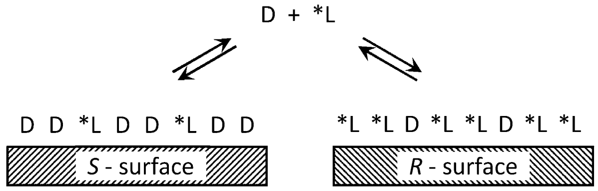

Figure 2. Adsorbed D- and *L-enantiomers on chiral surfaces at equilibrium with a racemic mixture in the gas phase. The higher adsorption energy of the D-enantiomer on the *S*-surface results in a higher coverage of the D-enantiomer than the *L-enantiomer (left). As a result of the diastereomeric relationship between the adsorption energies, the *L-enantiomer has a higher coverage than the D-enantiomer on the *R*-surface (right).

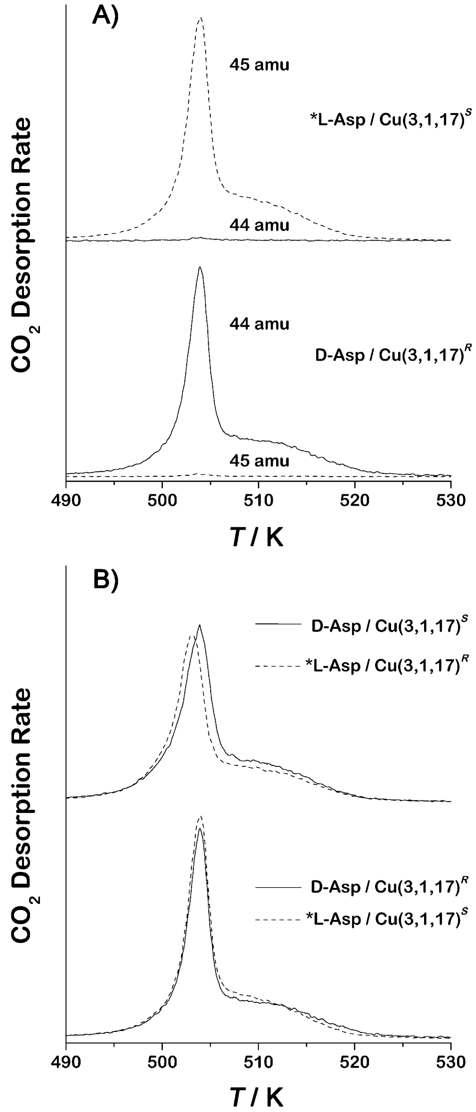

Figure 3. Temperature-programmed reaction spectroscopy (TPRS) of D- and *L-Asp on the Cu(3,1,17)$^{R\&S}$ surfaces at saturation coverage. A) Monitoring of CO_2 ($m/q = 44$ amu) and *CO_2 ($m/q = 45$ amu) clearly differentiates enantiomers. B) Equivalent combinations of adsorbate and substrate show no isotope effect on the decomposition kinetics.

This work has used the adsorption of D- and L-aspartic acid on the Cu(3,1,17)$^{R\&S}$ surfaces under ultra-high vacuum conditions for quantitative measurement of enantiospecific adsorption equilibrium constants. For the purpose of enantiodifferentiation, we have used *L-aspartic acid-1,4-$^{13}C_2$ ($HO_2{}^{13}CCH(NH_2)CH_2{}^{13}CO_2H$, hitherto *L-Asp) and unlabeled D-aspartic acid (D-Asp). By analogy with the surface chemistry of tartaric acid and other amino acids on Cu surfaces, we expect that Asp is singly deprotonated ($^{-}O_2CCH(NH_2)CH_2CO_2H$) at high coverages.[4b,d] On Cu(3,1,17)$^{R\&S}$ surfaces, Asp adsorbs irreversibly in the sense that it decomposes during heating to yield CO_2 and $N{\equiv}CCH_3$ as gas phase products. The yields of $^{13}CO_2$ (45 amu) and CO_2 (44 amu) can be used for enantiodiscrimination of adsorbed *L-Asp and D-Asp and determination of their relative coverages (Figure 3A). There is no measurable isotope effect or enantiospecificity to the decomposition kinetics on Cu(3,1,17)$^{R\&S}$ (Figure 3B).

During competitive adsorption, displacement of adsorbed molecules by gas phase molecules establishes equilibrium. During initial exposure of a clean surface to a gas phase racemic mixture, the coverages of the two enantiomers both increase in proportion to their gas phase concentrations and their sticking coefficients. Once the surface is saturated with adsorbed species, the components displace one another to establish equilibrium between the gas phase and the adsorbed phase. One of the critical characteristics of D- and *L-Asp adsorption on Cu(3,1,17)$^{R\&S}$ is that they displace one another on time scales that allow equilibrium to be achieved. In Figure 4A the Cu(3,1,17)^{S} surface was saturated with *L-Asp at 400 K and then held at 460 K while being exposed to a flux of D-Asp for various lengths of time. After each exposure, the adsorbed Asp mixture was decomposed by heating while measuring the yields of CO_2 and $^{13}CO_2$ to determine the relative coverages of D- and *L-Asp. After 50 min exposure to D-Asp, most of the *L-Asp was displaced from the surface while the total coverage of D- and *L-Asp remained constant. The exponential decay and growth curves fitted to the data yield a displacement rate constant of $k_S^{*L\rightarrow D} = 1.05(\pm 0.04) \times 10^{-3}\,s^{-1}$. In Figure 4B the Cu(3,1,17)^{S} surface was saturated with D-Asp and then exposed to a flux of *L-Asp. Again one observes displacement but with a smaller displacement rate constant of $k_S^{D\rightarrow *L} = 0.37(\pm 0.01) \times 10^{-3}\,s^{-1}$. Similar enantiospecific displacement kinetics have been observed recently using chiral Au nanoparticles.[6] Our data imply that the aspartic acid is adsorbed in a molecular state at 460 K and suggest that the enantiospecific binding energy of D-Asp on the Cu(3,1,17)^{S} surface is greater than that of *L-Asp.

In order to study enantioselective adsorption, Cu(100) and Cu(3,1,17)$^{R\&S}$ surfaces at 460 K were exposed to a racemic mixture of D,*L-Asp for increasing periods of time. To control the D-/*L-Asp flux ratio, the temperatures of the glass vials containing *L-Asp and D-Asp were controlled independently. After exposure of the surfaces to the gas phase racemic mixture, the ratio of D-/*L-Asp coverages, θ^{D}/θ^{*L}, was determined from the CO_2 and $^{13}CO_2$ yields during heating and plotted as $\ln(\theta^{D}/\theta^{*L})$ versus exposure time in Figure 5.

As expected, Figure 5 shows that the ratio of adsorbed D- and *L-Asp coverages on the achiral Cu(100) surface (★)

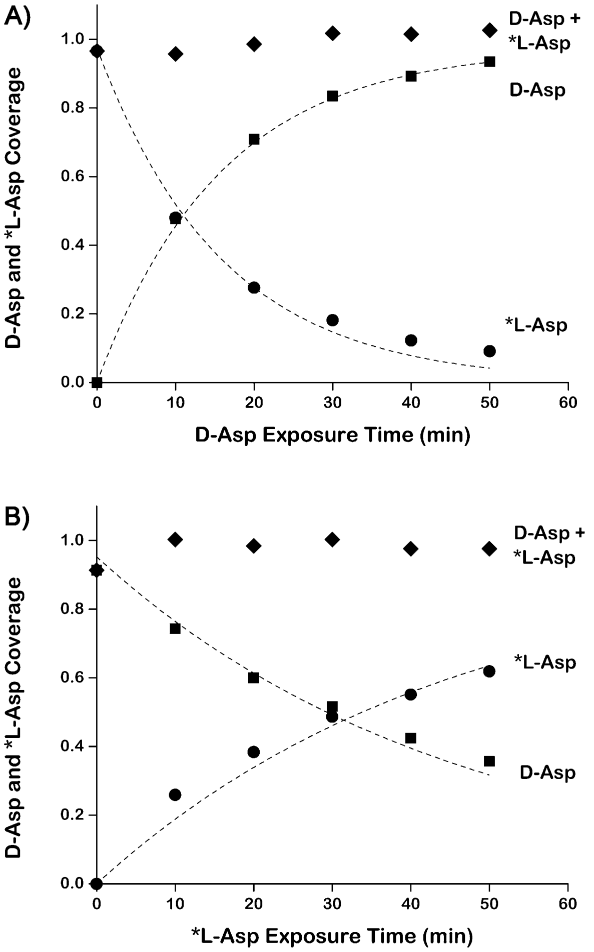

Figure 4. Mutual displacement of D-Asp and *L-Asp on the Cu(3,1,17)^S surface at 460 K. A) Displacement of *L-Asp during exposure to D-Asp. B) Displacement of D-Asp during exposure to *L-Asp. The curves are exponential decay and growth functions. The rate constant for displacement of *L-Asp by D-Asp is $k_S^{*\mathrm{L}\rightarrow\mathrm{D}} = 1.05(\pm 0.04)\times 10^{-3}\ \mathrm{s}^{-1}$ while the rate constant for displacement of D-Asp by *L-Asp is $k_S^{\mathrm{D}\rightarrow *\mathrm{L}} = 0.37(\pm 0.01)\times 10^{-3}\ \mathrm{s}^{-1}$. These enantiospecific time constants indicate that D-Asp has a higher binding energy on Cu(3,1,17)^S than *L-Asp.

remains unity for all exposure times. Until the Cu(3,1,17)^R surface becomes saturated (< 20 min), the coverages of adsorbed D- and *L-Asp (●) are equal because the fluxes of D- and *L-Asp and their sticking coefficients are equal. During continued exposure for > 20 min, *L-Asp displaces D-Asp until $\theta_R^{\mathrm{D}}/\theta_R^{*\mathrm{L}} = 0.53$ after 80 min. In order to determine whether the apparent asymptote of the ratio is representative of equilibrium, the Cu(3,1,17)^R surface was first prepared with a saturated layer of Asp with $\theta_R^{\mathrm{D}}/\theta_R^{*\mathrm{L}} = 0.32$, enriching the surface with *L-Asp beyond equilibrium. During subsequent exposure to racemic D,*L-Asp, the coverage ratio increased to $\theta_R^{\mathrm{D}}/\theta_R^{*\mathrm{L}} = 0.40$ (▲), suggesting that the equilibrium coverage ratio lies between the two asymptotic values of 0.40 and 0.53. When the Cu(3,1,17)^R surface was first prepared with a saturated layer of Asp with $\theta_R^{\mathrm{D}}/\theta_R^{*\mathrm{L}} = 0.46 \pm 0.02$ and then exposed to racemic D,*L-Asp, the coverage ratio (◆) remained constant. On the Cu(3,1,17)^S surface, the equilibrium value of $\theta_S^{\mathrm{D}}/\theta_S^{*\mathrm{L}}$ (○ and ◇) is 2.30 ± 0.06, the inverse of the ratio on the Cu(3,1,17)^R surface. This reflects the diastereomeric relationship between the adsorption energies of D- and *L-Asp on Cu(3,1,17)$^{R\&S}$ surfaces. These adsorption equilibrium constants are consistent with the displacement kinetics (Figure 4). Those suggest that on Cu(3,1,17)^S adsorption of D-Asp is energetically favored over adsorption of *L-Asp. Additional displacement experiments were performed using the source temperatures to achieve flux ratios of $F_{\mathrm{D}}/F_{*\mathrm{L}} = 2$ and $^1/_2$ (Supporting Information, Figures S1 and S2). For all three flux ratios ($F_{\mathrm{D}}/F_{*\mathrm{L}} = 2, 1$, and $^1/_2$) exposed to the Cu(3,1,17)$^{R\&S}$ surfaces $K_S^{\mathrm{D}}/K_S^{*\mathrm{L}} = K_R^{*\mathrm{L}}/K_R^{\mathrm{D}} = 2.29 \pm 0.17$ (Table 1). This is similar to the ratio of the displacement rate constants measured on Cu(3,1,17)^S (Figure 4), $k_S^{*\mathrm{L}\rightarrow\mathrm{D}}/k_S^{\mathrm{D}\rightarrow *\mathrm{L}} = 2.84 \pm 0.15$, in spite of the fact that those were measured under conditions far from equilibrium.

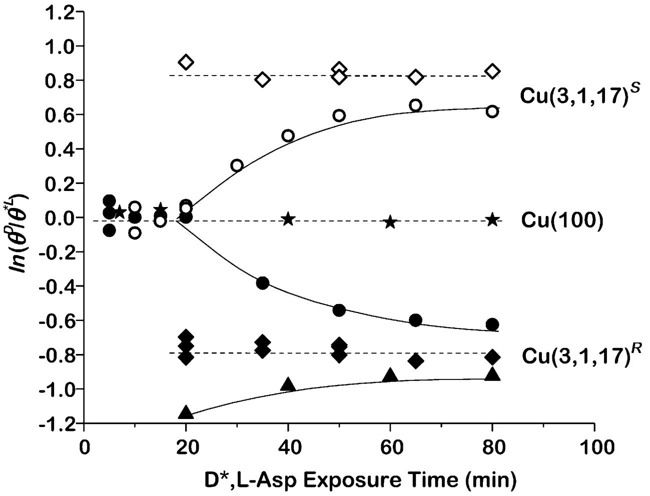

Figure 5. The Asp coverage ratios, $\ln(\theta^{\mathrm{D}}/\theta^{*\mathrm{L}})$, on Cu(3,1,17)$^{R\&S}$ and on Cu(100) at 460 K as a function of exposure time to racemic D*L-Asp. During the control experiment on the achiral Cu(100) surface, $\theta^{\mathrm{D}}/\theta^{*\mathrm{L}} = 1.0$ (★) for all exposure times. On the Cu(3,1,17)^R surface, the coverage ratio tends towards $\theta^{\mathrm{D}}/\theta^{*\mathrm{L}} = 0.46$ when starting with initial coverage ratios of 1.0 (●), 0.32 (▲) and 0.46 (◆). On the Cu(3,1,17)^S surface, the coverage ratio tends towards $\theta^{\mathrm{D}}/\theta^{*\mathrm{L}} = 2.3$ when starting with initial coverage ratios of 1.0 (○) and 2.3 (◇).

At equilibrium the relative coverages of the two enantiomers are determined by the competitive adsorption isotherm.

Table 1: The equilibrium coverage ratios of D-Asp to *L-Asp, equilibrium constant ratios, enantiomeric excess, and the enantiospecific difference in adsorption energies for equilibrium adsorption of D- and *L-Asp mixtures on Cu(3,1,17)$^{R\&S}$.

D-/*L-Asp flux ratio in the gas phase	Cu(3,1,17) surface chirality	$\theta^{\mathrm{D}}/\theta^{*\mathrm{L}}$	$K_R^{*\mathrm{L}}/K_R^{\mathrm{D}}$ or $K_S^{\mathrm{D}}/K_S^{*\mathrm{L}}$	*ee* [%][a]	$\Delta\Delta G$ [kJ mol^{-1}]
1.00	*R*	0.46	2.18	37	2.98
	S	2.30	2.30	39	3.18
0.50	*R*	0.17	2.39	41	3.33
	S	1.01	2.03	34	2.70
2.00	*R*	0.85	2.53	43	3.56
	S	4.58	2.29	39	3.17

[a] To compare enantiomeric excess for three different mixtures, the values were calculated based on the equilibrium constants ratios.

For a Langmuir isotherm, the coverage ratios of D- and *L-Asp on Cu(3,1,17)^S are given by Eq. (1):

$$\frac{\theta_S^{\mathrm{D}}}{\theta_S^{*\mathrm{L}}} = \frac{K_S^{\mathrm{D}}}{K_S^{*\mathrm{L}}}\frac{P_{\mathrm{D}}}{P_{*\mathrm{L}}} = \frac{K_S^{\mathrm{D}}}{K_S^{*\mathrm{L}}}\frac{F_{\mathrm{D}}}{F_{*\mathrm{L}}} = \frac{F_{\mathrm{D}}}{F_{*\mathrm{L}}}\exp\left(\frac{\Delta\Delta G}{RT}\right) \tag{1}$$

where K is the adsorption equilibrium constant, and P is the gas phase partial pressure of each enantiomer which is proportional to the flux, F, in our experiments. The quantity $\Delta\Delta G$ is the enantiospecific difference in the adsorption free energies.

The coverage ratios of D- and *L-Asp on Cu(3,1,17)$^{R\&S}$ surfaces, the estimated ratios of equilibrium constants and the estimated values of $\Delta\Delta G$ are summarized in Table 1 for all six combinations of gas phase fluxes and surfaces. The enantiomeric excess and the enantiospecific difference in adsorption energies are $ee = 39 \pm 3\,\%$ and $\Delta\Delta G = 3.15 \pm 0.29\ \mathrm{kJ\,mol^{-1}}$, respectively. These favor adsorption of D-Asp on the Cu(3,1,17)^S surface and *L-Asp on the Cu(3,1,17)^R surface. The ability to measure enantiomeric excess with high accuracy also results in accurate measurement of the enantiospecific difference in adsorption energy. The method allows a truly differential measurement of adsorption energies, in spite of the fact that one cannot measure the adsorption energy of either enantiomer directly.

This work represents the first unequivocal evidence of enantioselective, equilibrium separation of a racemic mixture on a naturally chiral metal surface. The enantioselectivity in this case is much higher than that of chiral molecules on mineral surfaces, most of which yield enantioselectivities of 1–2 %.[1d,2b,e,f] Furthermore, the quantitative nature of the ^{13}C labeling method has provided the first direct measure of an enantiospecific adsorption energy difference on a chiral metal surface. Its application to other amino acids and to other naturally chiral metal surface structures offers an opportunity to study chiral surface chemistry with the accuracy needed to provide a fundamental understanding of the origins of enantioselective surface chemistry.

Experimental Section

Study of enantiospecific adsorption of D- and *L-Asp on Cu(3,1,17)$^{R\&S}$ surfaces was performed in an ultrahigh vacuum system with a base pressure of 2×10^{-10} Torr. The chamber is equipped with an ion sputter gun for sample cleaning, low energy electron diffraction optics, and a mass spectrometer for TPD studies. The chirality of the Cu(3,1,17)$^{R\&S}$ surfaces was determined by X-ray diffraction.[5g] Before each experiment, the Cu samples were cleaned by 1 keV Ar$^+$ ion sputtering, annealing at 850 K for 500 s and then cooled at a controlled rate of $-1\ \mathrm{K\,s^{-1}}$ at a pressure of $< 1 \times 10^{-9}$ Torr. Unlabeled D-Asp (Sigma–Aldrich, 99 % chemical purity) and isotopically labeled *L-Asp (Cambridge Isotope Laboratories, 98 % chemical purity, 99 atom % 1,4-^{13}C$_2$) were sublimed onto the Cu surface from two glass vials. The fluxes of D- and *L-Asp from each evaporation source were controlled via the sublimation temperature (380–403 K). The exposure time was controlled by a shutter placed in front of the glass vial. After the exposure, the Cu sample was resistively heated from 250 K to 670 K at $1\ \mathrm{K\,s^{-1}}$ while the species desorbing from the surface were monitored by the mass spectrometer.

Received: November 12, 2012

Keywords: adsorption · asymmetric catalysis · chirality · enantioselectivity · surfaces

---

[1] a) W. A. Bonner, P. R. Kavasmaneck, F. S. Martin, J. J. Flores, *Origins Life* **1975**, *6*, 367 – 376; b) W. A. Bonner, *Origins Life Evol. Biosphere* **1991**, *21*, 59 – 111; c) J. L. Bada, *Nature* **1995**, *374*, 594 – 595; d) R. M. Hazen, D. S. Sholl, *Nat. Mater.* **2003**, *2*, 367 – 374.

[2] a) G. Karagunis, G. Coumoulos, *Nature* **1938**, *142*, 162 – 163; b) W. A. Bonner, P. R. Kavasmaneck, F. S. Martin, J. J. Flores, *Science* **1974**, *186*, 143 – 144; c) P. R. Kavasmaneck, W. A. Bonner, *J. Am. Chem. Soc.* **1977**, *99*, 44 – 50; d) H. H. Teng, P. M. Dove, C. A. Orme, J. J. De Yoreo, *Science* **1998**, *282*, 724 – 727; e) R. M. Hazen, T. R. Filley, G. A. Goodfriend, *Proc. Natl. Acad. Sci. USA* **2001**, *98*, 5487 – 5490; f) W. A. Bonner, P. R. Kavasmaneck, *J. Org. Chem.* **1976**, *41*, 2225 – 2226.

[3] I. Weissbuch, L. Leiserowitz, M. Lahav, *Isr. J. Chem.* **2011**, *51*, 1017 – 1033.

[4] a) C. J. Baddeley, *Top. Catal.* **2003**, *25*, 17 – 28; b) S. M. Barlow, R. Raval, *Surf. Sci. Rep.* **2003**, *50*, 201 – 341; c) M. Ortega Lorenzo, C. J. Baddeley, C. Muryn, R. Raval, *Nature* **2000**, *404*, 376 – 379; d) B. Behzadi, S. Romer, R. Fasel, K. H. Ernst, *J. Am. Chem. Soc.* **2004**, *126*, 9176 – 9177.

[5] a) C. F. McFadden, P. S. Cremer, A. J. Gellman, *Langmuir* **1996**, *12*, 2483 – 2487; b) G. A. Attard, A. Ahmadi, J. Feliu, A. Rodes, E. Herrero, S. Blais, G. Jerkiewicz, *J. Phys. Chem. B* **1999**, *103*, 1381 – 1385; c) G. A. Attard, *J. Phys. Chem. B* **2001**, *105*, 3158 – 3167; d) J. D. Horvath, A. J. Gellman, *J. Am. Chem. Soc.* **2001**, *123*, 7953 – 7954; e) D. S. Sholl, A. Asthagiri, T. D. Power, *J. Phys. Chem. B* **2001**, *105*, 4771 – 4782; f) J. D. Horvath, A. Koritnik, P. Kamakoti, D. S. Sholl, A. J. Gellman, *J. Am. Chem. Soc.* **2004**, *126*, 14988 – 14994; g) W. Y. Cheong, A. J. Gellman, *J. Phys. Chem. C* **2011**, *115*, 1031 – 1035.

[6] S. Knoppe, R. Azoulay, A. Dass, T. Burgi, *J. Am. Chem. Soc.* **2012**, *134*, 20302 – 20305.